Two-neutron transfer in nuclei close to the drip line

E. Khan,[1] N. Sandulescu,[2,3] Nguyen Van Giai,[1] and M. Grasso[1]
[1]*Institut de Physique Nucléaire, IN_2P_3-CNRS, 91406 Orsay, France*
[2]*Institute for Physics and Nuclear Engineering, P.O. Box MG-6, 76900 Bucharest, Romania*
[3]*Royal Institute of Technology, SCFAB, SE-10691 Stockholm, Sweden*
(Received 22 May 2003; published 30 January 2004)

We investigate the two-neutron transfer modes induced by (t, p) reactions in neutron-rich oxygen isotopes. The nuclear response to the pair transfer is calculated in the framework of continuum quasiparticle random phase approximation (cQRPA). The cQRPA allows a consistent determination of the residual interaction and an exact treatment of the continuum coupling. The (t, p) cross sections are calculated within the distorted wave Born approximation approach and the form factors are evaluated by different methods: macroscopically, following the Bayman and Kallio method, and fully microscopically. A significant part of the cross section corresponds to a high-lying collective mode built entirely upon continuum quasiparticle states.

DOI: 10.1103/PhysRevC.69.014314 PACS number(s): 21.60.Jz, 25.60.Je, 21.10.Re

I. INTRODUCTION

Two-neutron transfer reactions such as (t, p) or (p, t) have been used for many years in order to study the nuclear pairing correlations (for a recent review see Ref. [1]). The corresponding pair transfer modes are usually described in terms of pairing vibrations or pairing rotations [2,3].

High-energy collective pairing modes, called giant pairing vibrations (gpv), were also predicted [4,5], but they have not been observed yet. Recently there is a renewed interest for the study of two-neutron transfer reactions with weakly bound exotic nuclei. These reactions would provide valuable information about the pairing correlations in nuclei far from stability. The use of two-neutron transfer reactions with exotic nuclei can also increase the chance of exciting the gpv mode, as discussed recently in Ref. [6].

The two-particle transfer modes are commonly described by the particle-particle (pp) random phase approximation [7,8] in the case of closed shell nuclei and by the quasiparticle random phase approximation (QRPA) [3,6] in open shell nuclei. Most of the cross section calculations use the distorted wave Born approximation (DWBA). The form factor is usually calculated by means of macroscopic models [9,10] or by using the Bayman and Kallio method [11]. Several aspects of the model are under discussion, especially for absolute cross section calculations [12]: one-step or sequential two-step process, triton wave function, zero-range or finite-range DWBA. The so-called 0*S* [13] approximation is also generally used to calculate the cross section in the DWBA framework. In the latter approximation, the QRPA solutions act as a spectroscopic factor [3], therefore the microscopic information does not affect the shape of the form factor.

The calculation of the two-particle transfer modes in nuclei far from stability presents additional difficulties compared to the case of stable nuclei. One of such difficulties is related to the continuum coupling, which becomes important in nuclei close to the drip lines. Therefore in nuclei close to the drip lines the pair transfer, the ground state properties, and the continuum coupling should be calculated consistently. The aim of this paper is to present such a consistent description of the two-particle transfer in the framework of the continuum-QRPA (cQRPA) approach recently developed in Ref. [14]. In the cQRPA the continuum is treated exactly and the residual interaction is derived from the same effective force used in the Hartree-Fock-Bogoliubov (HFB) approximation for calculating the ground state properties. In this way the fluctuations of the particle and pairing densities, which are coupled together in the cQRPA, are calculated on the same footing with the ground state densities.

The paper is organized as follows. In Sec. II we present the cQRPA model and show how the response function for the two-particle transfer is calculated within this model. In Sec. III we discuss the response function for the particular case of two neutrons transferred to the neutron-rich oxygen isotopes. In Sec. IV we present the calculation of cross sections for the transfer reaction $^{22}\mathrm{O}(t, p)$.

II. THE CONTINUUM-QRPA AND THE TWO-PARTICLE RESPONSE

Due to the concept of quasiparticle (qp), the QRPA unifies on the same ground the particle-hole (ph) RPA and the pp-RPA with the inclusion of the pairing effects. In the continuum-QRPA model, presented in detail in Ref. [14], the response of the nuclear system to an external perturbation is obtained from the time-dependent HFB (TDHFB) equations [15]

$$i\hbar\frac{\partial\mathcal{R}}{\partial t} = [\mathcal{H}(t) + \mathcal{F}(t), \mathcal{R}(t)], \tag{1}$$

where $\mathcal{R}$ and $\mathcal{H}$ are the time-dependent generalized density and the HFB Hamiltonian, respectively. $\mathcal{F}$ is the external oscillating field,

$$\mathcal{F} = Fe^{-i\omega t} + \text{H.c.} \tag{2}$$

In Eq. (2) F includes both particle-hole and two-particle transfer operators,

$$F = \sum_{ij} F_{ij}^{11} c_i^\dagger c_j + \sum_{ij} (F_{ij}^{12} c_i^\dagger c_j^\dagger + F_{ij}^{21} c_i c_j), \tag{3}$$

and $c_i^\dagger$, c_i are the particle creation and annihilation operators, respectively.

In the small amplitude limit the TDHFB equations become

$$\hbar\omega \mathcal{R}' = [\mathcal{H}', \mathcal{R}^0] + [\mathcal{H}^0, \mathcal{R}'] + [F, \mathcal{R}^0], \tag{4}$$

where the prime stands for the corresponding perturbed quantity. The variation of the generalized density $\mathcal{R}'$ is expressed in term of three quantities, namely, ρ', κ', and $\bar{\kappa}'$, which are written as a column vector,

$$\boldsymbol{\rho}' = \begin{pmatrix} \rho' \\ \kappa' \\ \bar{\kappa}' \end{pmatrix}, \tag{5}$$

where $\rho'_{ij} = \langle 0 | c_j^\dagger c_i | ' \rangle$ is the variation of the particle density, $\kappa'_{ij} = \langle 0 | c_j c_i | ' \rangle$ and $\bar{\kappa}'_{ij} = \langle 0 | c_j^\dagger c_i^\dagger | ' \rangle$ are the fluctuations of the pairing tensor associated with the pairing vibrations and $|'\rangle$ denotes the change of the ground state wave function $|0\rangle$ due to the external field. In contrast with the RPA where one needs to know only the change of the ph density (ρ'), the variation of the three quantities (5) has to be calculated in the QRPA. In the three dimensional space introduced in Eq. (5), the first dimension represents the ph subspace, the second the particle-particle (pp) one, and the third the hole-hole (hh) one. The response matrix has therefore nine coupled elements in QRPA, compared to one in the RPA formalism.

The variation of the HFB Hamiltonian is given by

$$\boldsymbol{\mathcal{H}}' = \mathbf{V}\boldsymbol{\rho}', \tag{6}$$

where $\mathbf{V}$ is the matrix of the residual interaction expressed in terms of the second derivatives of the HFB energy functional, namely,

$$\mathbf{V}^{\alpha\beta}(\mathbf{r}\sigma, \mathbf{r}'\sigma') = \frac{\partial^2 E}{\partial \rho_{\bar{\beta}}(\mathbf{r}'\sigma')\, \partial \rho_{\bar{\alpha}}(\mathbf{r}\sigma)}, \quad \alpha, \beta = 1, 2, 3. \tag{7}$$

In the above equation the notation $\bar{\alpha}$ means that whenever α is 2 or 3 then $\bar{\alpha}$ is 3 or 2.

Introducing for the external field the three dimensional column vector

$$\mathbf{F} = \begin{pmatrix} F^{11} \\ F^{12} \\ F^{21} \end{pmatrix}, \tag{8}$$

the density changes can be written in the standard form

$$\boldsymbol{\rho}' = \mathbf{G}\mathbf{F}, \tag{9}$$

where $\mathbf{G}$ is the QRPA Green's function obeying the Bethe-Salpeter equation,

$$\mathbf{G} = (1 - \mathbf{G}_0\mathbf{V})^{-1}\mathbf{G}_0 = \mathbf{G}_0 + \mathbf{G}_0\mathbf{V}\mathbf{G}. \tag{10}$$

The unperturbed Green's function $\mathbf{G}_0$ has the form

$$\mathbf{G}_0{}^{\alpha\beta}(\mathbf{r}\sigma, \mathbf{r}'\sigma'; \omega) = \sum\!\!\!\!\!\!\int_{ij} \frac{\mathcal{U}_{ij}^{\alpha 1}(\mathbf{r}\sigma)\bar{\mathcal{U}}_{ij}^{*\beta 1}(\mathbf{r}'\sigma')}{\hbar\omega - (E_i + E_j) + i\eta} - \frac{\mathcal{U}_{ij}^{\alpha 2}(\mathbf{r}\sigma)\bar{\mathcal{U}}_{ij}^{*\beta 2}(\mathbf{r}'\sigma')}{\hbar\omega + (E_i + E_j) + i\eta}, \tag{11}$$

where E_i are the qp energies and $\mathcal{U}_{ij}$ are 3×2 matrices expressed in term of the two components of the HFB wave functions [14]. The $\sum\!\!\!\!\!\!\int$ symbol in Eq. (11) indicates that the summation is taken both over the discrete and the continuum qp states.

The QRPA Green's function can be used for calculating the strength function associated with various external perturbations. For instance, the transitions from the ground state to the excited states induced by a particle-hole external field can be described by the strength function

$$S(\omega) = -\frac{1}{\pi}\mathrm{Im}\int F^{11*}(\mathbf{r})\mathbf{G}^{11}(\mathbf{r}, \mathbf{r}'; \omega)F^{11}(\mathbf{r}')d\mathbf{r}\, d\mathbf{r}', \tag{12}$$

where $\mathbf{G}^{11}$ is the (ph,ph) component of the QRPA Green's function. Examples of such calculations can be found in Ref. [14].

The quantity of interest in this work is the strength function describing the two-particle transfer from the ground state of a nucleus with A nucleons to the excited states of a nucleus with $A+2$ nucleons. This strength function is

$$S(\omega) = -\frac{1}{\pi}\mathrm{Im}\int F^{12*}(\mathbf{r})\mathbf{G}^{22}(\mathbf{r}, \mathbf{r}'; \omega)F^{12}(\mathbf{r}')d\mathbf{r}\, d\mathbf{r}', \tag{13}$$

where $\mathbf{G}^{22}$ denotes the (pp,pp) component of the Green's function.

III. PAIR TRANSFER IN OXYGEN ISOTOPES: STRENGTH FUNCTIONS

In the cQRPA model presented above one should calculate in the first step the ground state of the system within the continuum-HFB (cHFB) approach [16]. The cHFB equations are solved in coordinate space assuming spherical symmetry. In the cHFB calculations presented here the mean field quantities are evaluated using the Skyrme interaction SLy4 [17], while for the pairing interaction we take a zero-range density-dependent force. The parameters of the pairing force used here for calculating the neutron-rich oxygen isotopes are taken the same as in Ref [14]. These parameters are fixed for a model space determined by a qp energy cutoff equal to 50 MeV and a maximum angular momentum $j = 9/2$. The HF single-particle and HFB qp energies corresponding to the *sd* shell and to the $1f_{7/2}$ state are listed in Table I. In both HF and cHFB calculations the state $1f_{7/2}$ is a wide resonance for $^{18-22}$O nuclei, while the state $1d_{3/2}$ is a narrow resonance.

In the cQRPA calculations we include the full discrete and continuum qp spectrum up to 50 MeV. These states, which generate a two-quasiparticle spectrum with a maximum energy of 100 MeV, are used to construct the unperturbed

TABLE I. ^{18,20,22}O single-particle and single-quasiparticle neutron energies calculated in the Hartree-Fock and the continuum-HFB models, respectively. The Skyrme interaction used is SLy4 and the resonances are displayed in brackets (energy;width).

		^{18}O	^{20}O	^{22}O
$1d_{5/2}$	HF	−6.7	−7.0	−7.45
$1d_{5/2}$	cHFB	2.26	2.08	2.30
$2s_{1/2}$	HF	−4.0	−4.2	−4.6
$2s_{1/2}$	cHFB	3.46	2.28	1.05
$1d_{3/2}$	HF	(0.46;0.02)	(0.51;0.03)	(0.42;0.02)
$1d_{3/2}$	cHFB	(7.74;0.12)	(6.60;0.29)	(5.39;0.01)
$1f_{7/2}$	HF	(5.50;1.35)	(5.24;1.24)	(4.86;1.04)
$1f_{7/2}$	cHFB	(12.77;1.13)	(12.14;0.83)	(10.05;0.69)

Green's function $\mathbf{G}_0$. The residual interaction is derived from the two-body force used in cHFB according to Eq. (2.7). The contribution given by the velocity-dependent terms of the Skyrme force to the residual interaction is calculated in the Landau-Migdal approximation. Due to this approximation the self-consistency of the HFB+QRPA equations is not exactly preserved in the numerical calculations. Therefore, the spurious mode associated with the center-of-mass motion is not at zero energy. In order to put this spurious mode to zero energy we renormalize in the cQRPA calculations the Skyrme force by 20% for all the oxygen isotopes. In addition to this spurious mode, there is also a spurious Goldstone mode connected to the particle number, which is conserved only in average in the HFB approximation. This spurious mode is fixed to zero energy by changing the strength of the pairing force by a small amount, of maximum 5% for all the calculated isotopes. The strength function for the two-neutron transfer is calculated using Eq. (13). For the radial function $F^{22}(r)$ we take the form r^L, which is equal to the unity for the $L=0$ pair transfer mode considered here [6]. The unperturbed Green's function is calculated with an averaging interval η equal to 0.15(1.0) MeV for excitations energies below (above) 11 MeV.

The results for the strength function corresponding to a neutron pair transferred to the oxygen isotopes ^{18,20,22}O are shown in Fig. 1. The exact continuum treatment is also compared to box discretization calculations (the box radius is 22.5 fm, and the averaging interval η is 0.15 MeV). The first

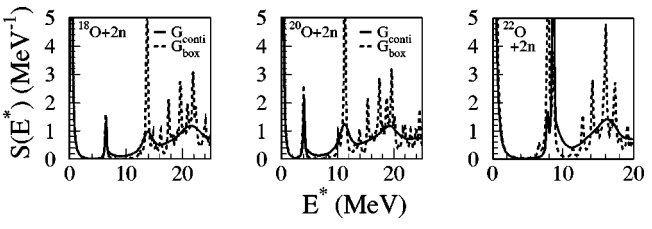

FIG. 1. The QRPA response for the two-neutron transfer on ^{18,20,22}O. The exact continuum calculations are in solid lines whereas the calculations with box boundary conditions are in dashed lines. The results are displayed as functions of E^*, the excitation energy with respect to the final nucleus ground state.

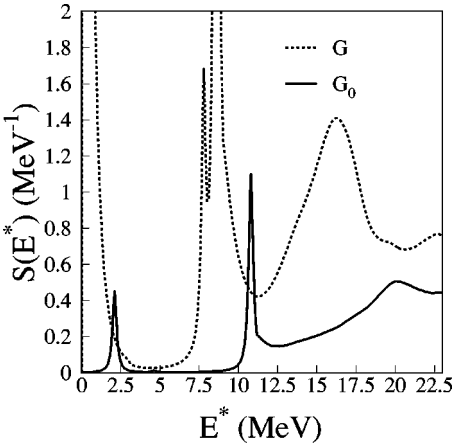

FIG. 2. The response function for the two-neutron transfer on ^{22}O. The unperturbed response is in solid line and the QRPA response in dashed line.

intense peak located at zero energy corresponds to the pair transfer to the collective Goldstone mode associated with particle number fluctuations. For the isotopes ^{18,20}O the next two peaks located at higher energy correspond to a pair transferred mainly to the states $2s_{1/2}$ and $1d_{3/2}$, respectively. For the isotope ^{22}O, the peak located around 8.6 MeV corresponds to a pair transferred mainly to the states $1d_{3/2}$. For all the isotopes we can see a broad resonant structure around 20 MeV which is built mainly upon the single-particle resonant state $1f_{7/2}$. This two-quasiparticle broad resonance has the characteristics of a giant pairing vibration [4–6]. It should be noted that the continuum treatment affects the magnitude of low energy states for the three responses. This is due to the collective nature of these states, since unbound configurations such as the $(1d_{3/2})^2$ contribute to these low-lying states. This points to the necessity to use exact continuum calculations even to predict transitions towards low-lying states. The state at 8.6 MeV on the ^{22}O+2n spectrum is embedded in the continuum and it is naturally more affected by the continuum treatment. The influence of the residual interaction on the pair transfer modes is illustrated in Fig. 2 for the case of ^{22}O+2n, emphasizing the collective nature of the pairing vibrations [3]. As expected, the residual interaction shifts down the position of the two-quasiparticle resonant state located at 10.8 MeV in the G_0 response and increases its strength. This peak in the G_0 response corresponds to the addition of two neutron qp on the $(1d_{3/2})^2$ subshell. Apart from that, we can also notice a sensitive change in the spreading widths of the two-quasiparticle resonant states when the residual interaction is turned on. Thus, due to the mixing of the configurations $(1f_{7/2})^2$ and $(1d_{3/2})^2$ by the residual interaction, the broad peak around 18 MeV becomes narrower and the narrow peak around 10 MeV becomes wider. This is a general effect which appears whenever in the two-body wave functions wide and narrow single-particle resonant states are mixed together [18].

IV. PAIR TRANSFER IN OXYGEN ISOTOPES: CROSS SECTIONS

The DWBA calculation of the cross section for the two-neutron transfer requires the form factor, which represents

TABLE II. The parameters of the optical potential [21,22] used for the transfer reaction ^{22}O(t, p) at 15 MeV/nucleon. V is the depth used for the real part of the potential, W for the imaginary absorptive part, W_s for the surface imaginary part, and V_{so} for the spin-orbit part. The depths are given in MeV and the radii and diffuseness parameters in fm.

	V	r_0	a_0	W	r_W	a_W	W_S	r_{W_S}	a_{W_S}	V_{so}	r_{so}	a_{so}
^{22}O$+t$	156	1.20	0.72	28	1.40	0.84	0	0	0	2.5	1.20	0.72
^{24}O$+p$	50.6	1.17	0.75	5.9	1.32	0.74	6.0	1.32	0.74	6.2	1.01	0.75

the correlation between the two neutrons and the initial nucleus [19]. In order to compare the influence of various approximations, the form factor is calculated below by three different ways: macroscopically, by the so-called Bayman and Kallio method, and using the cQRPA model. The calculations based on the cQRPA allow for a straightforward study of the effects of the pairing correlations and of the continuum coupling upon the cross section. The form factors and the cross sections will be calculated below for the particular transfer reaction ^{22}O(t, p).

A. The macroscopic form factor

In Refs. [9,10] the form factor is calculated from the variation of the optical potential U with respect to the change of the number of particles:

$$F(r) = \beta_p \frac{dU}{dA}, \tag{14}$$

where β_p is the so-called pairing deformation parameter representing the strength of the two-neutron pairing transfer reaction.

Using for the nuclear radius the relation $R = r_0 A^{1/3}$ one gets

$$F(r) = \beta R \frac{dU}{dr}, \tag{15}$$

where

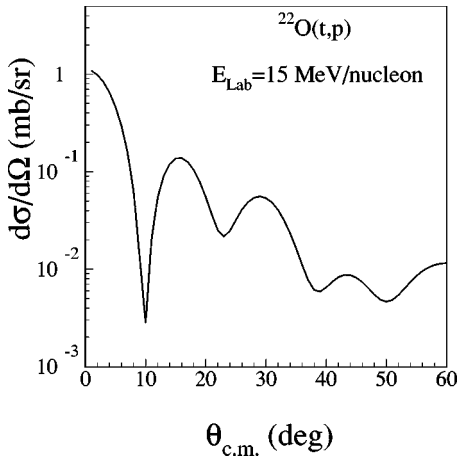

FIG. 3. DWBA calculations for the reaction ^{22}O(t, p) at 15 MeV/nucleon calculated with a macroscopic form factor (see text for details).

$$\beta = \frac{\beta_p}{3A}. \tag{16}$$

Equation (15) is referred to the macroscopic form factor.

In this model for the form factor the transfer is considered as an inelastic process corresponding to a deformation parameter given by Eq. (16). One advantage of this model is that the two-particle transfer cross section can be calculated by knowing only the optical potential in the entrance channel. It should be stressed that Eq. (14) assumes that the optical potential changes smoothly with the number of nucleons. Therefore, one expects that this model for the form factor works better for heavy nuclei.

The cross section for the reaction ^{22}O(t, p) is calculated in the DWBA approximation using the ECIS88 code [20]. The reaction energy is chosen to be 15 MeV/nucleon. For the optical potential corresponding to the system ^{22}O$+t$ we use the potential derived by Becchetti and Greenlees [21]. The parameters corresponding to this potential are summarized in Table II. The β_p parameter associated with a particular transfer mode is obtained by taking the average of the square root of the integral of the strength function over the energy region corresponding to that mode. The calculations are performed for the peak located at 8.6 MeV and for the broad resonant region located around 16 MeV. The angular distribution corresponding to the state located at 8.6 MeV, displayed in Fig. 3, is showing a typical diffraction pattern. For the other state the pattern of the angular distribution is the same. The only difference is in their magnitude, which depends on the β_p value. Table III shows the total cross sections obtained for the two states mentioned above. The continuum treatment affects the cross section by 10% to 20%.

B. The Bayman and Kallio form factor

Bayman and Kallio have proposed a method to calculate the form factor on a semimicroscopic ground. In this method

TABLE III. Total cross section (mb) of the ^{22}O(t, p) reaction at $E = 15$ MeV/nucleon. The calculations are performed for the resonant states of the ^{22}O$+2n$ system located at 8.6 MeV and for the giant pairing vibration (gpv) mode. The results are obtained using the macroscopic model for the form factor [1]. The first (second) row shows the results obtained with box (continuum) boundary conditions.

	$E = 8.6$ MeV	gpv
Box	0.353	0.523
Continuum	0.281	0.455

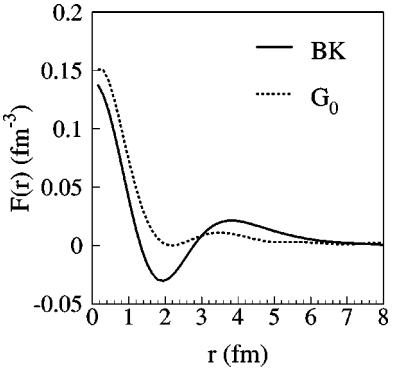

FIG. 4. The microscopic form factors for the lowest energy state in the ^{22}O+2n system. The solid line is obtained using the Bayman and Kallio method, and the dashed line with the unperturbed $\mathbf{G}_0$ response.

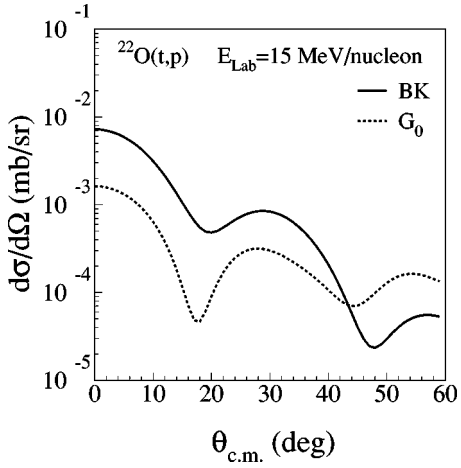

FIG. 5. 15 MeV/nucleon ^{22}O(t, p) DWBA calculations using the form factors shown in Fig. 4.

the two-particle wave function of the transferred pair is expressed in term of the single-particle wave functions corresponding to a Woods-Saxon potential [11]. The spectroscopic factors of the single-particle states are an input of the calculation. An example of such calculation for the form factor is shown in Fig. 4 The calculation is for the configuration $(2s_{1/2})^2$ and for the ^{22}O+2n system. The Woods-Saxon potential was obtained by the separation energy method, where the depth of the potential is set in order to reproduce the binding energy of the single particle to the core. The radius and the diffuseness of the potential were taken at the standard values of 1.25 fm and 0.65 fm, respectively. For the spectroscopic factor of the single-particle state we take the value 1. As can be seen in Fig. 4, the Bayman and Kallio form factor has also negative values. This is due to the fact that in this calculation the two neutrons are not considered at the same position in the two-neutron wave function.

The previous ^{22}O+t Becchetti and Greenlees optical potential [21] is used for the entrance channel and the ^{22}O+p Becchetti and Greenlees [22] for the exit channel, in order to calculate the DWBA cross section. The resulting optical potential parameters are given in Table II. The DWBA calculations are performed with the DWUCK4 [23] code and using the zero-range approximation. In this approximation the two-neutrons and the residual fragment are located at the same point and the range function is expressed through a simple constant D_0 [19]. For the (t, p) reaction we take D_0=2.43 $\times 10^4$ MeV^2 fm^3 [24]. This value relies on measurements of the $2n+p$ system and may be subject to uncertainties [19]. The angular distribution for the (t, p) reaction at E =15 MeV/nucleon obtained with the Bayman and Kallio form factor is shown in Fig. 5. As discussed in Refs. [3,12,19], the shape of the angular distribution is usually described correctly by the zero-range approximation, but not its magnitude, which is generally underestimated by a large amount. Therefore in what follows we will focus our discussion not on the absolute values of the cross sections, but rather on the relative values obtained using different form factors.

C. The microscopic form factor

In the nuclear response theory the transition from the ground state to the excited state $|\nu\rangle$ of the same nucleus is determined by the transition density defined by

$$\rho^{\nu}(\mathbf{r}\sigma) = \langle 0|c^{\dagger}(\mathbf{r}\sigma)c(\mathbf{r}\sigma)|\nu\rangle, \tag{17}$$

where $c^{\dagger}(\mathbf{r}\sigma)$ is the particle creation operator in coordinate space. The corresponding quantity for describing pair transfer processes is the pair transition density defined by

$$\kappa^{\nu}(\mathbf{r}\sigma) = \langle 0|c(\mathbf{r}\bar{\sigma})c(\mathbf{r}\sigma)|\nu\rangle, \tag{18}$$

where $c^{\dagger}(\mathbf{r}\bar{\sigma}) = -2\sigma c^{\dagger}(\mathbf{r}-\sigma)$ is its time reversed counterpart. The pair transition density defined above determines the transition from the ground state of a nuclei with A nucleons to a state $|\nu\rangle$ of a nucleus with $A+2$ nucleons. This quantity is the output of cQRPA calculations. The form factor for the pair transfer is obtained by folding the pair transition density κ^{ν} [Eq. (18)] with the interaction acting between the transferred pair and the residual fragment [1]. In the zero-range approximation used here the dependence of this interaction on the relative distance between the pair and the fragment is taken as a delta force. Therefore in this approximation the pair transition density (18) coincides with the form factor [19].

Figure 4 displays the pair transition density corresponding to the lowest energy state of the final nucleus in the ^{22}O +2n system, derived from the $\mathbf{G}_0$ response, i.e., without taking into account the residual interaction between the quasiparticles. Thus the dashed curve corresponds to a pair transferred in the pure two-quasiparticle configuration $(2s_{1/2})^2$ and is directly comparable to the Bayman and Kallio form factor, shown by the full line, corresponding also to the addition of a pair of neutrons in a pure two-particle configuration $(2s_{1/2})^2$. As can be seen in Fig. 4, the form factor derived from the $\mathbf{G}_0$ response has at large distances a smaller amplitude compared to the Bayman and Kallio form factor. This is due to the occupancy of the state $2s_{1/2}$, which is different from zero in the case of the $\mathbf{G}_0$ response. Another reason is that in the pair transition density given by Eq. (18) the two

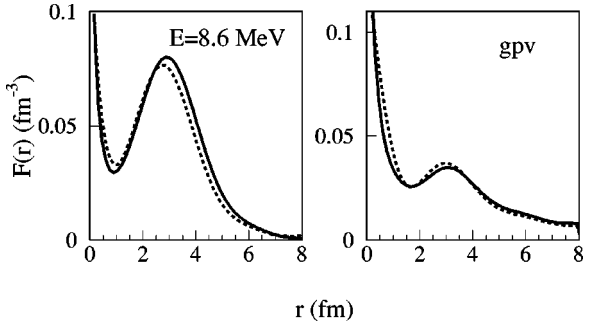

FIG. 6. The QRPA form factors for the 8.6 MeV state and for the giant pairing vibration region. The form factors obtained with box boundary conditions are in solid lines whereas the form factors obtained with the exact continuum treatment are displayed in dashed lines. The calculations are done for the $^{22}O+2n$ system.

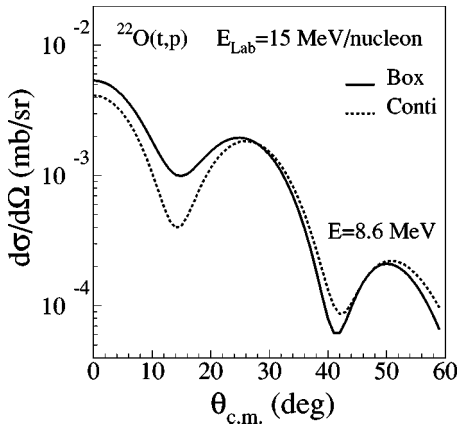

FIG. 7. DWBA calculations for the 8.6 MeV state. The solid (dashed) line corresponds to the QRPA results obtained with box (exact) boundary conditions. The calculations correspond to the system $^{22}O+2n$.

neutrons are taken to be at the same position whereas in the Bayman and Kallio method the two neutrons are allowed to be at different positions.

Figure 5 displays the angular distributions for the reaction $^{22}O(t,p)$ at 15 MeV/nucleon. The optical potential we have used in calculations is the same as above. The angular distributions are mainly sensitive to the surface part of the form factor, where the form factors calculated with the Bayman and Kallio method and with $\mathbf{G}_0$ show strong variations. The diffraction minima are shifted by around five degrees between the two calculations. The angular distribution calculated with the Bayman and Kallio form factor drops faster with increasing angle. This is due to the spatial extension of the two transferred neutrons which produces the negative part of the form factor. In order to see the continuum effect on the form factor, in Fig. 6 we display the transition densities calculated by solving the QRPA equations with continuum and box-type asymptotic conditions, for the mode located at 8.6 MeV and for the giant pairing vibrations. The corresponding effect on the (t,p) angular distribution is illustrated in Fig. 7 for the state located at 8.6 MeV. The effect is large for this state, which is built mainly upon narrow resonant qp states: the angular distributions are mainly sensitive to the surface of the form factor. From Fig. 6 we can see that the continuum treatment has also some effect on the form factor corresponding to the high energy mode around 16 MeV, especially at small values of the nuclear radius. However, its effect on the global cross section remains negligible, about 3%.

V. CONCLUSIONS

In this paper we have investigated the pair transfer in neutron-rich oxygen isotopes in the framework of the continuum-QRPA. The form factors are calculated with a macroscopic model, the Bayman and Kallio approach, and fully microscopically. The cross section is evaluated by using the DWBA and the zero-range approximation. The response function exhibits some narrow resonances corresponding to a pair transfer in the single-particle states of *sd* shell and a broad peak at high energies. This peak is built mainly upon the single-particle resonance $1f_{7/2}$ and its cross section is much larger than the one associated with the lower energy transfer modes. Since this high energy transfer mode is formed mainly by single-particle states above the valence shell, this mode is similar to the giant pairing vibration mode suggested long ago. Although such a mode has not been detected yet, the pair transfer reactions involving exotic loosely bound nuclei may offer a better chance for this undertaking. On the theoretical side, one needs to make a better estimation for the absolute cross section associated with this mode. Due to the collectivity of the final states the continuum treatment has also an impact on low-lying states. The form factors calculated microscopically show an effect of the continuum treatment on the form factor for high energy states. The angular distributions are mainly affected in their diffraction minima for narrow high energy states. In the case of the gpv, no drastic influence of the exact continuum treatment is observed. It should be interesting to perform the DWBA calculations without the zero-range approximation in order to make more quantitative predictions for the cross section. This requires to fold the pair transition densities with the interaction between the two neutrons and the residual fragment.

ACKNOWLEDGMENTS

E.K. acknowledges fruitful discussions with S. Fortier and J. Van de Wiele. N.S. thanks Roberto Liotta for useful discussions on giant pairing vibrations and the Swedish Foundation for International Cooperation in Research and Higher Education (STINT) for financial support.

[1] W. von Oertzen and A. Vitturi, Rep. Prog. Phys. **64**, 1247 (2001).
[2] D. R. Bès and R. A. Broglia, Nucl. Phys. **80**, 289 (1966).
[3] R. A. Broglia, O. Hansen, and C. Riedel, Adv. Nucl. Phys. **6**, 287 (1973).
[4] R. A. Broglia and D. R. Bès, Phys. Lett. **69B**, 129 (1977).
[5] M. W. Herzog, R. J. Liotta, and T. Vertse, Phys. Lett. **165B**, 35 (1985).
[6] L. Fortunato, W. von Oertzen, H. M. Sofia, and A. Vitturi, Eur. Phys. J. A **14**, 37 (2002).
[7] A. Bouyssy and N. Vinh Mau, Nucl. Phys. **A224**, 331 (1974).
[8] G. Ripka and R. Padjen, Nucl. Phys. **A132**, 489 (1969).
[9] C. H. Dasso and G. Pollarolo, Phys. Lett. **155B**, 223 (1985).
[10] C. H. Dasso and A. Vitturi, Phys. Rev. Lett. **59**, 634 (1987).
[11] B. F. Bayman and A. Kallio, Phys. Rev. **156**, 1121 (1967).
[12] M. Igarashi, K. Kubo, and K. Yagi, Phys. Rep. **199**, 1 (1991).
[13] R. A. Broglia, C. Riedel, and T. Udagawa, Nucl. Phys. **A169**, 225 (1971).
[14] E. Khan, N. Sandulescu, M. Grasso, and N. V. Giai, Phys. Rev. C **66**, 024309 (2002).
[15] P. Ring and P. Schuck, *The Nuclear Many-Body Problem* (Springer-Verlag, Berlin, 1980).
[16] M. Grasso, N. Sandulescu, Nguyen Van Giai, and R. J. Liotta, Phys. Rev. C **64**, 064321 (2001).
[17] E. Chabanat, P. Bonche, P. Haensel, J. Meyer, and R. Schaeffer, Nucl. Phys. **A635**, 231 (1998).
[18] R. Id Betan, R. J. Liotta, N. Sandulescu, and T. Vertse, Phys. Rev. Lett. **89**, 042501 (2002).
[19] G. R. Satchler, *Direct Nuclear Reactions* (Clarendon, Oxford, 1983).
[20] J. Raynal, Phys. Rev. C **23**, 2571 (1981).
[21] F. D. Becchetti and G. W. Greenlees, in *Polarization Phenomena in Nuclear Reactions*, edited by H. H. Barschall and W. Haeberti (The University of Wisconsin Press, Madison, 1971), p. 682.
[22] F. D. Becchetti and G. W. Greenlees, Phys. Rev. **182**, 1190 (1969).
[23] P. D. Kunz, program DWUCK4, University of Colorado (unpublished).
[24] J. Van de Wiele (private communication).